

## Defect formation and phase stability of $\text{Cu}_2\text{ZnSnS}_4$ photovoltaic material

Akihiro Nagoya and Ryoji Asahi  
Toyota Central R&D Laboratories, Inc., Nagakute, Aichi 480-1192, Japan

Roman Wahl and Georg Kresse

Faculty of Physics and Center for Computational Materials Science, Universität Wien, Sensengasse 8/12, A-1090 Wien, Austria

(Received 22 September 2009; revised manuscript received 23 February 2010; published 15 March 2010)

First-principles studies of the phase stability of and defect formation in  $\text{Cu}_2\text{ZnSnS}_4$  (CZTS) are performed. We show that CZTS is the thermodynamically stable phase for a rather small confined domain of chemical potentials. Even slight deviations from the optimal growth conditions will therefore result in the formation of other sulfidic precipitates, including ZnS,  $\text{Cu}_2\text{SnS}_3$ , SnS,  $\text{SnS}_2$ , and CuS. In particular, under the prevalent experimental Cu-poor and Zn-rich growth conditions ZnS is the main competing phase. Furthermore, the calculations unambiguously predict that Cu at the Zn site is the most stable defect in the entire stability range of CZTS. This correlates with the experimental observation that CZTS is an intrinsic  $p$ -type semiconductor.

DOI: [10.1103/PhysRevB.81.113202](https://doi.org/10.1103/PhysRevB.81.113202)

PACS number(s): 71.15.Mb, 71.55.-i, 72.40.+w

The quaternary semiconductor  $\text{Cu}_2\text{ZnSnS}_4$  (CZTS) has drawn much interest as an absorber layer in thin-film solar cells, because its constituents are nontoxic and abundant in the earth's crust.<sup>1-16</sup> The CZTS thin films possess kesterite ( $\bar{I}4$ ) structure and show  $p$ -type conductivity, a direct band gap of 1.4–1.5 eV, and a high optical absorption of  $10^4 \text{ cm}^{-1}$ .<sup>4-7,9,13,17</sup> The highest conversion efficiency of CZTS reported so far is 6.7%,<sup>2</sup> demanding further improvement for practical applications. Cu-poor [ $\text{Cu}/(\text{Zn}+\text{Sn}) \sim 0.85$ ] and Zn-rich [ $\text{Zn}/\text{Sn} \sim 1.25$ ] conditions are often used in experiment to achieve a better solar cell performance.<sup>2,10-12</sup> Under these conditions, intrinsic defects and/or precipitates of other phases are to be anticipated. It is thus necessary to understand the nature of these defects in CZTS in order to improve the solar cell performance. However, there have been only a few discussions of defects in CZTS, in contrast to the much more popular ternary photovoltaic materials such as  $\text{CuInSe}_2$  and  $\text{CuGaSe}_2$ . Very recently, during the reviewing procedure of the present Brief Report, a study on the defect formation of CZTS has been reported.<sup>8</sup> They suggested that Cu-rich/Zn-poor conditions are necessary for the growth of the single-phase CZTS and reported the defect formation energies under such a condition. In this Brief Report we employ first-principles calculations to determine the stability of intrinsic point defects under comprehensive conditions where the parent material is in thermal equilibrium and stable against competing phases.

The calculations were performed using the plane-wave projector augmented-wave method<sup>18,19</sup> applying the Perdew-Burke-Ernzerhof (PBE) exchange-correlation functional<sup>20</sup> as implemented in the Vienna *ab initio* simulation package (VASP).<sup>21,22</sup> A plane-wave cutoff of 300 eV was used. To determine accurate formation energies of defects in the dilute limit, we calculated formation energies for different supercells, i.e., up to 512 atoms/cell as described below. The lattice constants were fixed at the optimized ones for the perfect CZTS crystal,<sup>6</sup> while the ionic positions were relaxed until the residual forces became less than 0.2 eV/Å. Band filling corrections and multipole corrections were performed for finite supercells as discussed below.<sup>23,24</sup> We confirmed that the

non-spin-polarized state is always stable for all considered defects. Although the calculated band gap by PBE was 0.1 eV, much lower than the experimental value,<sup>6</sup> the band-gap correction was not included since we assumed  $p$ -type CZTS and thus unimportance of accurate evaluation of donor states.

The formation energy for a defect  $D$  in a charge state  $q$ ,  $\Delta H_{D,q}$ , is expressed by<sup>23,25</sup>

$$\Delta H_{D,q}(E_F, \mu) = (E_{D,q} - E_p) + \sum_{\alpha} n_{\alpha} \mu_{\alpha} + q(E_v + E_F), \quad (1)$$

where  $E_{D,q}$  and  $E_p$  are the total energies of CZTS with and without defect  $D$ , respectively, and  $E_F$  is the Fermi energy of the system measured from the valence-band maximum (VBM)  $E_v$ . The equilibrium concentration of the defect  $D$  in the charge state  $q$  will be proportional to the Boltzmann factor  $\exp[-\Delta H_{D,q}(E_F, \mu)/k_B T]$ . We assumed  $p$ -type character for CZTS; hence,  $E_F$  was fixed at the VBM ( $E_F=0$ ). Since we are interested in the dilute defect limit,  $E_v$  was set to the value of the VBM in the perfect CZTS crystal. The atom index  $\alpha$  determines which atom is added or removed for the defect  $D$ , with  $n_{\alpha}=1$  if an atom is removed, while  $n_{\alpha}=-1$  if an atom is added. The chemical potentials  $\mu_{\alpha}$  are referenced to the standard elemental state, i.e.,  $\mu_{\alpha} = \mu_{\alpha}^0 + \Delta\mu_{\alpha}$ , where the reference potentials  $\mu_{\alpha}^0$  are those of metallic Cu, Zn, and Sn, and the solid state of S.

The allowed  $\Delta\mu_{\alpha}$  can be determined by the requirement that CZTS must be more stable than any competing phase, such as CuS (having symmetry  $P6_3/mmc$ ),  $\text{Cu}_2\text{S}$  ( $P4_32_12$ ), SnS ( $Pnma$ ),  $\text{SnS}_2$  ( $P\bar{3}m1$ ), ZnS ( $F\bar{4}3m$ ), and  $\text{Cu}_2\text{SnS}_3$  ( $Cc$ ). For a four-component system, three chemical potentials are independent, and one potential is fixed by the requirement that the stoichiometrically weighted sum of the chemical potentials should be equal to the total energy of the compound, i.e.,  $E_p = 2\mu_{\text{Cu}} + \mu_{\text{Zn}} + \mu_{\text{Sn}} + 4\mu_{\text{S}}$ . Using the heat of formation  $\Delta H(\text{CZTS})$ , and the chemical potentials referenced to the standard elemental states  $\Delta\mu_{\alpha}$ , the constraint can be written as

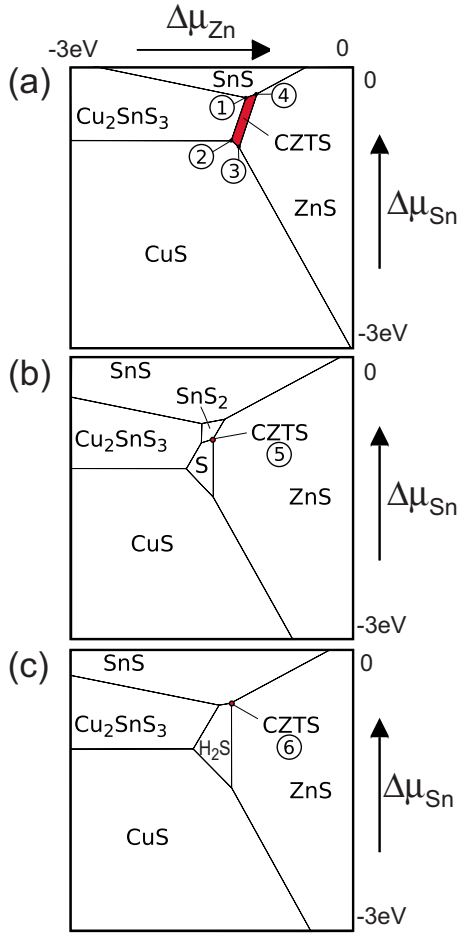


FIG. 1. (Color online) The chemical potential domains allowed for the CZTS phases (shown as the shaded areas and points) in the  $\Delta\mu_{\text{Zn}}$  and  $\Delta\mu_{\text{Sn}}$  planes for (a) Cu-rich conditions ( $\Delta\mu_{\text{Cu}}=0.0$  eV), (b) Cu-poor conditions ( $\Delta\mu_{\text{Cu}}=-0.41$  eV) using solid S as a sulfur source, and (c) Cu-poor conditions ( $\Delta\mu_{\text{Cu}}=-0.28$  eV) allowing for  $\text{H}_2\text{S}$  formation.

$$\Delta H(\text{CZTS}) = 2\Delta\mu_{\text{Cu}} + \Delta\mu_{\text{Zn}} + \Delta\mu_{\text{Sn}} + 4\Delta\mu_{\text{S}}. \quad (2)$$

The heat of formation of CZTS is calculated to be  $-3.2$  eV with respect to the elemental solids. This immediately yields lower and upper bounds for all chemical potentials, with  $\Delta\mu_{\alpha}$  confined by the relation  $-3.2 \leq \Delta\mu_{\alpha} \leq 0$  eV. To avoid the formation of competing phases, e.g.,  $\text{Cu}_2\text{SnS}_3$ , the chemical potentials are furthermore constrained by the following equation:

$$\Delta H(\text{Cu}_2\text{SnS}_3) \geq 2\Delta\mu_{\text{Cu}} + \Delta\mu_{\text{Sn}} + 3\Delta\mu_{\text{S}}, \quad (3)$$

and analogous constraints for other phases. In the first step, we determined the range of allowed chemical potentials, considering the other possible competing phases. We show in Fig. 1 two-dimensional slices of the phase stability diagram, for a fixed  $\Delta\mu_{\text{Cu}}$  and varying  $\Delta\mu_{\text{Zn}}$  and  $\Delta\mu_{\text{Sn}}$  values. For the Cu-rich conditions ( $\mu_{\text{Cu}}=0.0$ ), we find phase boundaries between CZTS and ZnS, SnS,  $\text{Cu}_2\text{SnS}_3$ , and CuS under Zn-rich, Sn-rich, Zn-poor, and Zn-poor and Sn-poor conditions, respectively. Even under Cu-rich conditions, CZTS is stable only in a very small regime of the phase diagram; in particu-

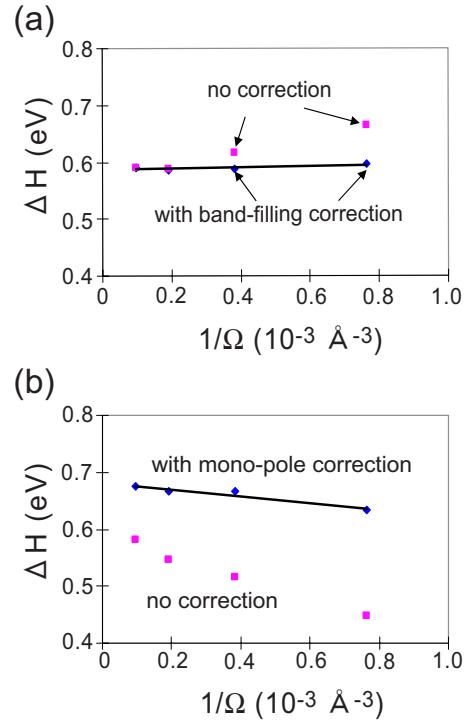


FIG. 2. (Color online) Formation energies of a Cu vacancy in CZTS with (a) band filling corrections for neutral cells (lines with dots) and (b) the monopole corrections for the charged ( $q=-1$ ) cells (lines with dots). Also shown are results without such corrections (dots).

lar,  $\mu_{\text{Zn}}$  must lie in a narrow range since CZTS competes with  $\text{Cu}_2\text{SnS}_3$  and ZnS. The situation becomes worse when the chemical potential of Cu is decreased (Cu-poor conditions). When only solid S is allowed as a competing phase, CZTS becomes unstable for  $\Delta\mu_{\text{Cu}} < -0.41$  eV [Fig. 1(b)], whereas if the formation of  $\text{H}_2\text{S}$  is allowed (e.g., if  $\text{H}_2$  is available), the stability regime is even smaller and CZTS becomes unstable for  $\Delta\mu_{\text{Cu}} < -0.28$  eV [Fig. 1(c)]. The very small phase stability regime of CZTS has profound implications for the growth process and implies that uttermost care must be used to avoid precipitates of the six competing solid phases. As often observed in experiment, one can take Cu-poor and Zn-rich conditions to avoid Zn-poor phases, such as  $\text{Cu}_2\text{SnS}_3$ ; but, unfortunately, in order to avoid the formation of ZnS precipitates, a relatively low Zn potential  $\Delta\mu_{\text{Zn}} < -1.0$  is required as well. On the other hand, the small stability regime allows an unambiguous determination which defects are the most stable ones in the stability regime of the parent CZTS compound.

In the second step, we determined the formation energies of point defects in the charged state  $q$ , considering vacancies of atoms at a site  $A$ ,  $(V \text{ at } A)^q$ , or a substitution of atom  $B$  for the atom at site  $A$ ,  $(B \text{ at } A)^q$ . We first demonstrate the accuracy and convergence of the present supercell calculations for a vacancy at the Cu site  $(V \text{ at } \text{Cu})$ . We employed supercells containing 64, 128, 256, and 512 atoms and used  $\Gamma$ -centered special  $\mathbf{k}$ -point sets with six, three, two, and one  $k$  point in the irreducible Brillouin zone, respectively. The  $k$ -point sets were chosen to be exactly identical and fold back

TABLE I. Formation energies (in eV) for possible point defects using chemical potentials at the CZTS domain boundaries specified in Fig. 1.  $E_F$  was fixed at the VBM. Those with the monopole corrections are listed in parentheses.

Defect	1	2	3	4	5	6
Cu at Zn	-0.164	-0.318	-0.252	-0.064	-0.121	-0.064
(Cu at Zn) <sup>-</sup>	-0.114 (0.001)	-0.268 (-0.153)	-0.202 (-0.087)	-0.015 (0.101)	-0.071 (0.044)	-0.015 (0.101)
(Zn at Cu) <sup>+</sup>	0.478 (0.593)	0.632 (0.747)	0.565 (0.680)	0.378 (0.493)	0.435 (0.550)	0.378 (0.493)
V at Cu	0.590	0.590	0.590	0.590	0.182	0.315
(V at Cu) <sup>-</sup>	0.591 (0.707)	0.591 (0.707)	0.591 (0.707)	0.591 (0.707)	0.183 (0.298)	0.316 (0.431)
Zn at Sn	0.599	0.291	0.158	0.532	0.419	0.532
Cu at Sn	0.698	0.236	0.170	0.732	0.562	0.732
V at Zn	0.785	0.631	0.697	0.885	0.420	0.609

to the same set in the Brillouin zone of the primitive cell. Gaussian smearing with a width of  $\sigma=0.02$  eV was used. Figure 2 shows the defect formation energies of the vacancy at the Cu site (V at Cu) as a function of  $1/\Omega$  (where  $\Omega$  is the cell volume) for the neutral and  $-1$  charged states, at Cu-rich conditions ( $\Delta\mu_{\text{Cu}}=0$ ). Figure 2(a) shows the neutral defect formation energy  $\Delta H_{V@Cu,0}$  with and without band filling corrections. Clearly, band filling corrections are indispensable for small supercells since the dispersion of the valence band is sizable.<sup>26</sup> After these corrections, the formation energy in the dilute limit ( $1/\Omega \rightarrow 0$ ) can be accurately predicted to be  $0.590 \pm 0.005$  eV. For charged defects, we first applied the monopole corrections<sup>24</sup> using the static dielectric constant of CZTS,  $\epsilon_0=10$ .<sup>6</sup> After these corrections  $\Delta H$  shows a residual linear error in  $1/\Omega$ , because of dipole-dipole interactions and elastic interactions between neighboring cells [see Fig. 2(b)]. Extrapolation to the dilute limit is, however, straightforward, and we obtained a well-converged formation energy of  $\Delta H_{V@Cu,-1}=0.681 \pm 0.007$  eV. We note, however, that including the monopole corrections usually yields an upper limit for the formation energy, in particular, if the defect charge is not localized.<sup>23,27</sup> For the present purpose we found the applied procedure to be sufficiently accurate using 64- and 128-atom cells, and we estimate the errors in the formation energies to be typically 20 meV using band filling and/or monopole corrections.

In Table I, we show the defect formation energies for various kinds of defects. The chemical potentials at the CZTS domain boundaries were used (marked by circles in Fig. 1). We list the results with and without monopole corrections, corresponding to the upper and lower bounds, but the results are essentially identical for both cases. The most stable defect is clearly and unambiguously Cu at Zn with a *negative formation energy for the entire allowed chemical potential range*. This implies the spontaneous formation of Cu antisite defects in the dilute limit, and since Cu has a valence of  $1+$  and Zn has a valence of  $2+$ , our result fully accounts for the *p*-type behavior usually observed in CZTS. Furthermore, Cu vacancies (V at Cu) under Cu-poor conditions (5), and Zn at Sn and Cu at Sn under the Sn-poor conditions (3) also exhibit relatively low formation energies of around 0.2 eV. We have also calculated all the possible interstitial defects among constituent elements. Their formation energies are however over 1 eV in the allowed chemical potential region.

To determine the formation energy of the Cu at Zn defect in the high concentration region, we determined the formation energies of Cu at Zn under Zn-rich conditions (points 4 or 6 in Fig. 1) using fully relaxed 128-, 64-, and 16-atom supercells, not employing band filling corrections. We found a roughly linear dependence of  $\Delta H$  on the inverse volume  $1/\Omega$ , becoming positive (endothermic) around a supercell volume of  $\Omega < 170 \text{ \AA}^3$  or a defect concentration larger than  $6 \times 10^{21} \text{ cm}^{-3}$ . This indicates that the antisite defect Cu at Zn in CZTS is thermodynamically stable up to fairly high concentrations. In practice, it would be quite important to control the Cu at Zn antisite concentration to optimize the carrier concentration in CZTS. One way is to employ Cu-poor and Zn-rich conditions or to introduce a compensating donor. This correlates with the experimental observation that Cu-poor and Zn-rich conditions help one to improve the solar cell performance, as already mentioned in the introduction.

Finally, to determine how these defects affect the electronic structure, we calculated the density of states (DOS) for a 64-atom supercell including a single defect. Figure 3 shows the results for the Cu at Zn and V at Cu defects compared to

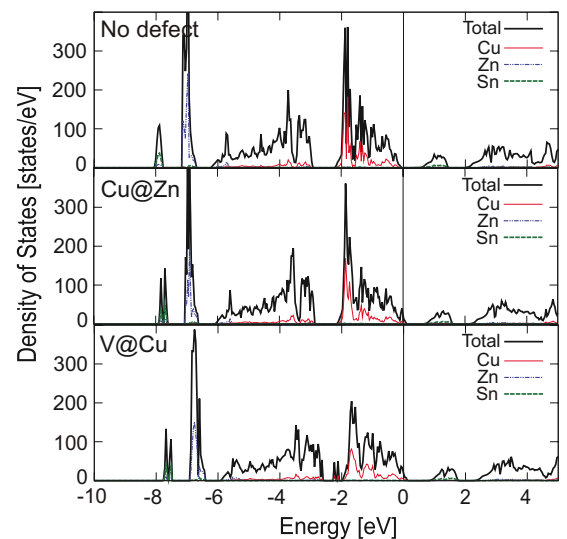


FIG. 3. (Color online) Densities of states of CZTS (upper panel) and 64-atom supercells with Cu at Zn (middle panel) and V at Cu (lower panel) defects. Partial densities of states projected into constituents are also shown.

that of defect-free CZTS, illustrating that these defects do not change the overall electronic structure but just place the Fermi energy at the VBM creating rather extended and shallow hole states. We also obtained similar DOSs for Zn at Sn and Cu at Sn. In particular, localized states deep in the CZTS band gap are not introduced by these defects. The avoidance of deep acceptors is a beneficial property of CZTS and implies that defects will not reduce the carrier mobility.

In conclusion, the defect formation energies of CZTS were calculated using first-principles calculations in the allowed range of the chemical potentials bounded by the precipitation conditions of the metal sulfides. Cu substitution at

the Zn site is the most stable defect and predicted to be even slightly exothermic in our case. It is without a question the dominant acceptor in *p*-type CZTS. CZTS is only stable for a small range of chemical potentials suggesting that synthesis is difficult since other sulfide precipitates might easily form; however, systematic control of defects and precipitation should provide a means to improve its crystallinity and solar cell performance.

This work was partially supported by the Austrian Fonds zur Förderung der wissenschaftlichen Forschung.

- 
- <sup>1</sup>H. Katagiri, N. Ishigaki, T. Ishida, and K. Saito, *Jpn. J. Appl. Phys., Part 1* **40**, 500 (2001).
- <sup>2</sup>H. Katagiri, K. Jimbo, S. Yamada, T. Kamimura, W. S. Maw, T. Fukano, T. Ito, and T. Motohiro, *Appl. Phys. Express* **1**, 041201 (2008).
- <sup>3</sup>H. Katagiri, K. Jimbo, W. Maw, K. Oishi, M. Yamazaki, H. Araki, and A. Takeuchi, *Thin Solid Films* **517**, 2455 (2009).
- <sup>4</sup>H. Matsushita, T. Maeda, A. Katsui, and T. Takizawa, *J. Cryst. Growth* **208**, 416 (2000).
- <sup>5</sup>J. J. Scragg, P. J. Dale, and L. M. Peter, *Electrochem. Commun.* **10**, 639 (2008).
- <sup>6</sup>J. Paier, R. Asahi, A. Nagoya, and G. Kresse, *Phys. Rev. B* **79**, 115126 (2009).
- <sup>7</sup>S. Chen, X. G. Gong, A. Walsh, and S. Wei, *Appl. Phys. Lett.* **94**, 041903 (2009).
- <sup>8</sup>S. Chen, X. G. Gong, A. Walsh, and S. Wei, *Appl. Phys. Lett.* **96**, 021902 (2010).
- <sup>9</sup>J.-S. Seol, S.-Y. Lee, J.-C. Lee, H.-D. Nam, and K.-H. Kim, *Sol. Energy Mater. Sol. Cells* **75**, 155 (2003).
- <sup>10</sup>K. Tanaka, M. Oonuki, N. Moritake, and H. Uchiki, *Sol. Energy Mater. Sol. Cells* **93**, 583 (2009).
- <sup>11</sup>H. Araki, A. Mikaduki, Y. Kubo, T. Sato, K. Jimbo, W. S. Maw, H. Katagiri, M. Yamazaki, K. Oishi, and A. Takeuchi, *Thin Solid Films* **517**, 1457 (2008).
- <sup>12</sup>A. Ennaoui *et al.*, *Thin Solid Films* **517**, 2511 (2009).
- <sup>13</sup>Y. B. Kishore Kumar, G. Suresh Babu, P. Uday Bhaskar, and V. Sundara Raja, *Sol. Energy Mater. Sol. Cells* **93**, 1230 (2009).
- <sup>14</sup>A. Weber, H. Krauth, S. Perlt, B. Schubert, I. Kötschau, S. Schorr, and H. W. Schock, *Thin Solid Films* **517**, 2524 (2009).
- <sup>15</sup>T. Todorov, M. Kita, J. Carda, and P. Escribano, *Thin Solid Films* **517**, 2541 (2009).
- <sup>16</sup>K. Oishi, G. Saito, K. Ebina, M. Nagahashi, K. Jimbo, W. S. Maw, H. Katagiri, M. Yamazaki, H. Araki, and A. Takeuchi, *Thin Solid Films* **517**, 1449 (2008).
- <sup>17</sup>K. Ito and T. Nakazawa, *Jpn. J. Appl. Phys., Part 1* **27**, 2094 (1988).
- <sup>18</sup>P. E. Blöchl, *Phys. Rev. B* **50**, 17953 (1994).
- <sup>19</sup>G. Kresse and D. Joubert, *Phys. Rev. B* **59**, 1758 (1999).
- <sup>20</sup>J. P. Perdew, K. Burke, and M. Ernzerhof, *Phys. Rev. Lett.* **77**, 3865 (1996).
- <sup>21</sup>G. Kresse and J. Furthmüller, *Comput. Mater. Sci.* **6**, 15 (1996).
- <sup>22</sup>G. Kresse and J. Furthmüller, *Phys. Rev. B* **54**, 11169 (1996).
- <sup>23</sup>C. Persson, Y.-J. Zhao, S. Lany, and A. Zunger, *Phys. Rev. B* **72**, 035211 (2005).
- <sup>24</sup>G. Makov and M. C. Payne, *Phys. Rev. B* **51**, 4014 (1995).
- <sup>25</sup>S. B. Zhang, S. H. Wei, A. Zunger, and H. Katayama-Yoshida, *Phys. Rev. B* **57**, 9642 (1998).
- <sup>26</sup>F. Oba, A. Togo, I. Tanaka, J. Paier, and G. Kresse, *Phys. Rev. B* **77**, 245202 (2008).
- <sup>27</sup>C. Freysoldt, J. Neugebauer, and C. G. Van de Walle, *Phys. Rev. Lett.* **102**, 016402 (2009).